International Journal of Modern Physics B
2150188 (16 pages)
© World Scientific Publishing Company
DOI: 10.1142/S0217979221501885

Numerical analysis of multiphase flow of couple stress fluid thermally effected by moving surface

Mubbashar Nazeer*, Farooq Hussain†, Fayyaz Ahmad‡, M. Ijaz Khan§, Fariha Gohar¶, M. Y. Malik‖, Tian-Chuan Sun**,†† and Adila Saleem¶

* *Department of Mathematics, Institute of Arts and Sciences, Government College University Faisalabad, Chiniot Campus, Chiniot 35400, Pakistan*

† *Department of Mathematical Sciences (FABS) BUITEMS, Quetta 87300, Pakistan*

‡ *Department of Applied Sciences, National Textile University, Faisalabad 38000, Pakistan*

§ *Department of Mathematics and Statistics, International Islamic University, Islamabad 44000 Pakistan*

¶ *Department of Mathematics, Riphah International University, Faisalabad 38000, Pakistan*

‖ *Department of Mathematics, College of Sciences, King Khalid University, Abha 61413, Saudi Arabia*

** *Qiuzhen College, Huzhou University, Huzhou 313000, P. R. China*
†† *ntch@zjhu.edu.cn*

Received 21 April 2021
Revised 26 May 2021
Accepted 27 May 2021
Published 31 July 2021

The study of multiphase flows gained much importance because of its extensive applications in nature and industry. These flows possess two or more thermodynamic phases, for example, one component phase (e.g., water vapors and water flow) or several components phase (e.g., water and oil flow). The most common example of multiphase flow in the context of the oil industry is petroleum. Further blood flow, porous structures, fluidized bed, bubbly flow in nuclear reactors, and fiber suspension in the paper industry are some significant examples of multiphase flows. In this paper, we considered the Couette flow of non-Newtonian (couple stress) fluid with variable magnetic field and thermal conductivity effects between parallel walls of the channel. The upper wall of the channel is in constant motion while the lower wall is in a fixed position. The variable viscosity effects with the suspension of hafnium particles are also discussed by taking

††Corresponding author.

Vogel's viscosity case. The shooting method based on the R–K method is applied to obtain the numerical solution of the current problem. A comparison between Newtonian and non-Newtonian fluids is presented by sketching graphs. The variations in flow and temperature of fluid against various involved factors, including variable viscosity, wall temperature, thermal radiations, variable magnetic field, and thermal conductivity are sketched and also physically described. It is observed that variable viscosity parameter elevated both velocity and temperature profiles while wall temperature parameter decelerated both fields. Further, noticed that the variable thermal conductivity and variable magnetic field impede the velocity of the fluid and also retarded the temperature field. Our attempt is not just useful to investigate the mechanical and industrial multiphase flows but also delivers important results to fill the gap in the existing literature.

Keywords: Two-phase flow; non-Newtonian fluid; variable magnetic field; Vogel's viscosity model; numerical scheme.

PACS numbers: 44.35.+c, 44.05.+e, 47.45.Gx, 47.60.+i

1. Introduction

Interest in non-Newtonian fluid flows with flexible liquid properties grown over the last few decades because of their sensitive behavior towards some properties like density, thermal conductivity, and viscosity to variation in heat produced as a result of internal frictional contacts.[1,2] That's why it is necessary to take measurements for the proper control of these variations. In this perspective, Qureshi *et al.*[3] addressed peristaltic transport with internal heat generation and radially magnetic field. Further, Bhatti and Zeeshan[4] explored the variations in non-Newtonian (blood flow) fluid by considering altering the values of magnetic field parameters. They also provided important results about friction forces and pressure in their work. The magnetohydrodynamics (MHD) effects on nanofluid (aluminum oxide nanoparticles and water-based fluid) were investigated by Hatami *et al.*[5] The variations in the flow of couple stress fluid against the variable magnetic field were explored by Hayat *et al.*[6] The study of MHD effects has several applications in industries involved electrically conducting fluids (plasmas, electrolytes, seawater, and molten metals) and in the medical field (hyperthermia, wound treatment with the help of magnetic field, compressor, and cancer treatment, etc.). Some important studies related to MHD effects on various non-Newtonian fluid flows are mentioned in Refs. 7–10. Several investigations revealed an important fact that fluid viscosity is strongly dependent on temperature, that is, the small change in temperature causes major variation in viscosity.[11–13] In most cases, when the viscosity of fluid decreases, this decrement causes an increase in fluid temperature. Hence for better heat and mass transfer performance, it is compulsory to adjust viscosity within a fluid by considering various temperature-dependent viscosity models like the Reynolds model and Vogel's model. The effects of variable viscosity on dusty fluid were examined by Manjunatha and Gireesha.[14] They discussed flow, temperature, Nusselt number, and skin-friction coefficient fields by sketching graphs. Castano *et al.*[15] examined Couette–Poiseuille flow with energy redistribution using large-Eddy simulation. The properties of heat transfer with variable viscosity for dusty fluid flow between parallel plates were discussed by Attia *et al.*[16] The electrically conducting flow of nanofluid with peristaltic motion through curved channel investigated by Ayub *et al.*[17] Some important investigations on variable viscosity and MHD effects are provided in Refs. 18–23.

Couple stress fluid is a significant non-Newtonian fluid that keeps "couple stress" properties. The flow characteristics of a couple stress fluids cannot be determined as they devise anti-symmetric stress tensors, but the study of such fluids is very advantageous to solve physical problems due to their major mechanical extent. These fluids have several uses in biochemical and mechanical industries. The main use of such fluids is in the lubrication of synovial linkages and investigation of peristalsis motion.[24–26] Different investigations revealed that the multiphase flow of couple stress fluids exhibits diverse rheological properties from common viscous fluids. The flows which possess two or more thermodynamic phases are categorized as multiphase flows. These phases may include one component (e.g., water vapors and water flow) or several components (e.g., water and oil flow). The compressible multiphase flow of gas-focused liquid was examined by Zahoor *et al.*[27] They provided the numerical simulation of gas-focused microjets and then compared results with experimental data. This study introduced new data about jet velocities of small-sized gas-focused nozzles. The multiphase slug flow through the capillary tube was investigated by Youn *et al.*[28] They calculated the effects of acceleration on the thickness of the liquid film by considering two-phase flow. The multiphase flow of gas–liquid interfaces was numerically and also experimentally explored by Zhang *et al.*[29] Liu *et al.*[30] evaluated the effects of surface roughness on multiphase flow. They used the lattice Boltzmann model to calculate the numerical solution. They concluded important results about the roughness of multiphase flows which are very helpful for further investigations about multiphase flows. Some recent studies on multiphase flows are cited in Refs. 31–34.

By keeping in mind the uses of couple stress multiphase flows with MHD effects, we investigated the Couette flow of non-Newtonian (couple stress) fluid with variable magnetic field and thermal conductivity between walls of the channel. The upper wall of the channel is in constant motion while the lower wall is in a fixed position. The variable viscosity effects are also discussed by taking Vogel's Viscosity case. A comparison between Newtonian and non-Newtonian fluids is presented by sketching graphs. Our attempt is not just useful to investigate the mechanical and industrial multiphase flows but also delivers important results to fill the gap in the existing literature.

2. Mathematical Analysis

Consider a Couette–Poiseuille flow of couple stress fluid between two parallel walls separated by distance $\pm\bar{h}$. The flow of fluid is examined in $(\bar{\eta}, \bar{\xi})$ plane as shown in Fig. 1. Here, the flow is unidirectional and the constant movement of the upper wall causes disturbance inflow along $\bar{\eta}$-direction.[35,36]

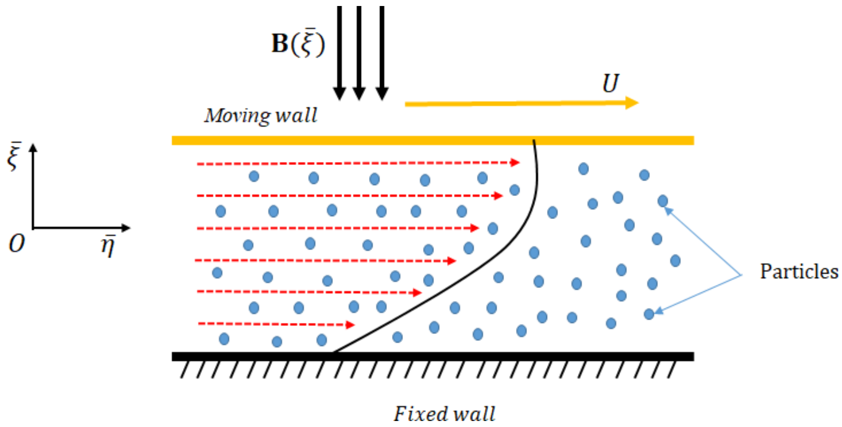

Fig. 1. (Color online) Two-phase flow.

The governing equations for couple stress fluid with the addition of hafnium particles[37,38] are discussed in the following.

2.1. *Flow equations*

The corresponding fluid phase and particle phase equations are, respectively,

$$\frac{\partial \bar{u}_f}{\partial \bar{\eta}} = 0, \tag{1}$$

$$\frac{\partial}{\partial \bar{\xi}}\left(\bar{\mu}_s \frac{\partial \bar{u}_f}{\partial \bar{\xi}}\right) - \bar{\xi}_1\left(\frac{\partial^4 \bar{u}_f}{\partial \bar{\xi}^4}\right) + \frac{\bar{C}\delta}{(1-\bar{C})}(\bar{u}_p - \bar{u}_f) - \frac{\bar{\sigma}\bar{B}^2(\bar{\xi})}{(1-\bar{C})}\bar{u}_f = \frac{\partial \bar{p}}{\partial \bar{\eta}}, \tag{2}$$

$$\frac{\partial \bar{u}_p}{\partial \bar{\xi}} = 0, \tag{3}$$

$$\bar{u}_f = \bar{u}_p + \frac{1}{\delta}\left(\frac{\partial k}{\partial \bar{\xi}}\right). \tag{4}$$

2.2. *Energy equation*

The corresponding energy equation for the present investigation can be written as

$$\bar{k}(\theta)\frac{\partial^2 \theta}{\partial \bar{\xi}^2} + \bar{\mu}_s\left(\frac{\partial \bar{u}_f}{\partial \bar{\xi}}\right)^2 - \frac{\partial q}{\partial \bar{\xi}} = \bar{\xi}_1\left(\frac{\partial \bar{u}_f}{\partial \bar{\xi}}\right)\left(\frac{\partial^3 U_f}{\partial \bar{\xi}^3}\right) - Q_0(\theta - \theta_0). \tag{5}$$

Tam[39] introduced the following drag coefficient of attraction:

$$\delta = \frac{4.5\bar{\mu}_0}{a}\bar{\lambda}(\bar{C}), \tag{6}$$

where a represents the radius of Hafnium particle and

$$\bar{\lambda}(\bar{C}) = \frac{4 + 3\sqrt{8\bar{C} - 3\bar{C}^2 + 3\bar{C}}}{(2 - 3\bar{C})^2}. \tag{7}$$

The variable viscosity, thermal radiation and thermal conductivity are specified by

$$\bar{\mu}_s = \bar{\mu}_0 e^{\frac{A}{B+\theta} - \theta_w}, \tag{8}$$

$$\frac{\partial q}{\partial \bar{\xi}} = -\frac{16\sigma^* \theta_0^3}{3k^*} \frac{\partial^2 \theta}{\partial \bar{\xi}^2}, \tag{9}$$

$$\bar{k} = k_0(1 + \beta_3 \theta). \tag{10}$$

2.3. *Corresponding boundary conditions*

$$\left.\begin{aligned} \bar{u}_f(\bar{\xi}) &= 0, \\ \frac{\partial^2 \bar{u}_f}{\partial \bar{\xi}^2} &= 0, \\ \theta(\bar{\xi}) &= \theta_0, \end{aligned}\right\}; \quad \text{where } \bar{\xi} = -\bar{h}, \tag{11}$$

$$\left.\begin{aligned} \bar{u}_f(\bar{\xi}) &= \bar{U}, \\ \frac{\partial^2 \bar{u}_f}{\partial \bar{\xi}^2} &= 0, \\ \theta(\bar{\xi}) &= \theta_w, \end{aligned}\right\}; \quad \text{where } \bar{\xi} = +\bar{h}. \tag{12}$$

Introducing the following normalized variables:

$$\begin{gathered} \bar{u}_f^* = \frac{\bar{u}_f}{U}; \quad \bar{u}_p^* = \frac{\bar{u}_p}{U}; \quad \eta^* = \frac{\eta}{h}; \quad \bar{\xi}^* = \frac{\bar{\xi}}{h}; \quad \bar{\mu}_s^* = \frac{\bar{\mu}_s}{\bar{\mu}_0}; \quad \bar{p}^* = \frac{h_p}{\bar{\mu}_0 U}; \\ \bar{B}_r = \frac{U^2 \bar{\mu}_0}{k(\theta_w \bar{-} \theta_0)}; \quad \bar{\gamma} = \sqrt{\frac{\bar{\mu}_0}{\eta^1}} h; \quad \bar{M} = \sqrt{\frac{\bar{\sigma}}{\bar{\mu}_0}} h \bar{B}_0; \quad \bar{m} = \frac{\bar{\mu}_0}{h^2 \delta}; \\ \theta^* = \frac{\theta - \theta_0}{\theta_w - \theta_0}; \quad \bar{u_s}^* = \frac{\bar{\mu}_s}{\bar{\mu}_0}; \quad \bar{k}^* = \frac{\bar{k}}{\bar{k}_0}. \end{gathered} \tag{13}$$

Equations (2) and (4) in normalized form, after ignoring asterisk, take the following forms:

$$\frac{d\bar{p}}{d\xi} = \frac{\partial}{\partial \bar{\xi}} \left(\bar{\mu}_s \frac{\partial \bar{u}_f}{\partial \bar{\xi}} \right) - \frac{1}{\bar{\gamma}^2} \left(\frac{d^4 \bar{u}_f}{d\bar{\xi}^4} \right) + \frac{\bar{C}}{\bar{m}} \frac{(\bar{u}_p - \bar{u}_f)}{(1 - \bar{C})} - \frac{\bar{M}^2 (1 + \beta_2 \xi)}{1 - \bar{c}} \bar{u}_f, \tag{14}$$

$$\bar{u}_p = \bar{u}_f - \bar{m} \frac{d\bar{p}}{d\bar{\xi}}. \tag{15}$$

The energy equation in normalized form can be expressed as

$$(1 + \beta_3 \theta + R_d) \frac{d^2 \theta}{d\bar{\xi}^2} + \bar{B}_r \bar{\mu}_s \left(\frac{d\bar{u}_f}{d\bar{\xi}} \right)^2 + q\theta = \frac{\bar{B}_r}{\bar{\gamma}^2} \left(\frac{d\bar{u}_f}{d\bar{\xi}} \right) \left(\frac{d^3 \bar{u}_f}{d\bar{\xi}^3} \right). \tag{16}$$

2.4. *Vogel's viscosity case*

Vogel's model is defined by[40–46]

$$\bar{\mu}_s(\theta) = \bar{\mu}_0 e^{\frac{A}{B+\theta} - \theta_w}. \tag{17}$$

By substituting Eqs. (15) and (17) in Eqs. (14) and (16), the following system of coupled nonlinear equations is obtained:

$$\frac{d^4\bar{u}_f}{d\bar{\xi}^4} - \bar{\gamma}^2\left(\frac{A}{(B+\theta)^2}\right)e^{\left(\frac{A}{B+\theta}-\theta_w\right)}\left(\frac{d\theta}{d\bar{\xi}}\frac{d\bar{u}_f}{d\bar{\xi}}\right) + \bar{\gamma}^2 e^{\left(\frac{A}{B+\theta}-\theta_w\right)}\frac{d^2\bar{u}_f}{d\bar{\xi}^2} + \frac{\bar{M}^2\bar{\gamma}^2(1+\beta_2\bar{\xi})}{(1-\bar{C})}\bar{u}_f + \frac{\bar{\gamma}^2\bar{p}}{(1-\bar{C})} = 0, \tag{18}$$

$$\frac{d^2\theta}{d\bar{\xi}^2} + \frac{\bar{B}_r}{(1+\beta_3\theta+R_d)}\left(e^{\left(\frac{A}{B+\theta}-\theta_w\right)}\right)\left(\frac{d\bar{u}_f}{d\bar{\xi}}\right)^2 + \frac{q\theta}{(1+\beta_3\theta+R_d)} = \frac{\bar{B}_r}{\bar{\gamma}^2(1+\beta_3\theta+R_d)}\left(\frac{d\bar{u}_f}{d\bar{\xi}}\right)\left(\frac{d^3\bar{u}_f}{d\bar{\xi}^3}\right). \tag{19}$$

Boundary conditions in the normalized form are

$$\left.\begin{aligned} \bar{u}_f(\bar{\xi}) &= 0,\\ \frac{\partial^2\bar{u}_f}{\partial\bar{\xi}^2} &= 0,\\ \theta(\bar{\xi}) &= 0, \end{aligned}\right\}; \quad \text{where } \bar{\xi} = -1, \tag{20}$$

$$\left.\begin{aligned} \bar{u}_f(\bar{\xi}) &= 1,\\ \frac{\partial^2\bar{u}_f}{\partial\bar{\xi}^2} &= 0,\\ \theta(\bar{\xi}) &= 1, \end{aligned}\right\}; \quad \text{where } \bar{\xi} = +1. \tag{21}$$

3. Numerical Method

In this investigation, the shooting method based on the R–K method[38] is applied to obtain the numerical solution of the current problem. The advantage of this method is that it is a fast converging and very efficient method based on the iterative scheme. In this method, the higher-order derivatives are reduced sequentially which decreases the error magnitude.

Consider the fluid phase velocity as

$$\bar{u}_f = \bar{f}_1. \tag{22}$$

The derivatives of the above equation in terms of ODE's can be expressed as

$$\bar{f}_2 = \frac{d\bar{u}_f}{d\bar{\xi}} = \bar{f}_1', \tag{23}$$

$$\bar{f}_3 = \frac{\partial^2\bar{u}_f}{\partial\bar{\xi}^2} = \bar{f}_2', \tag{24}$$

$$\bar{f}_4 = \frac{d^3\bar{u}_f}{d\bar{\xi}^3} = \bar{f}_3', \tag{25}$$

$$\bar{f}_5 = \theta, \tag{26}$$

$$\bar{f}_6 = \frac{d\theta}{d\bar{\xi}} = \bar{f}_5'. \tag{27}$$

The sign ($'$) in the above considerations symbolizes the derivative with respect to "$\bar{\xi}$". Hence the final expressions for fluid phase differential equations are

$$\begin{aligned}\bar{f}_4' = {} & \bar{\gamma}^2\bar{\beta}\left(\frac{A}{(B+\bar{f}_5)^2}\right)e^{\left(\frac{A}{B+\bar{f}_5}-\theta_w\right)}(\bar{f}_2\bar{f}_6) - \bar{\gamma}^2\bar{\beta}\left(\frac{A}{(B+\bar{f}_5)^2}\right)e^{\left(\frac{A}{B+\bar{f}_5}-\theta_w\right)}(\bar{f}_3)\\ & -\left(\frac{\bar{M}^2\bar{\gamma}^2(1+\beta_2\xi)}{(1-\bar{C})}\right)(\bar{f}_1) - \frac{\bar{\gamma}^2}{(1-\bar{C})}\bar{p},\end{aligned} \tag{28}$$

$$\bar{f}_6' = \frac{\bar{B}_r}{\bar{\gamma}^2(1+\beta_3\theta+R_d)}(\bar{f}_2)(\bar{f}_4). \tag{29}$$

Boundary conditions in view of the above suppositions are

$$\left.\begin{aligned}\bar{f}_1 &= 0,\\ \bar{f}_2 &= \bar{k}_1,\\ \bar{f}_3 &= 0,\\ \bar{f}_4 &= \bar{k}_2,\\ \bar{f}_5 &= 0,\\ \bar{f}_6 &= \bar{k}_3,\end{aligned}\right\}; \quad \text{when } \bar{\xi} = -1, \tag{30}$$

$$\left.\begin{aligned}\bar{f}_1 &= 1,\\ \bar{f}_2 &= \bar{k}_4,\\ \bar{f}_3 &= 0,\\ \bar{f}_4 &= \bar{k}_5,\\ \bar{f}_5 &= 1,\\ \bar{f}_6 &= \bar{k}_6,\end{aligned}\right\}; \quad \text{when } \bar{\xi} = +1, \tag{31}$$

where, $\bar{k}_1, \bar{k}_2, \bar{k}_3, \bar{k}_4, \bar{k}_5$ and $\bar{k}_6$ can be determined by using any suitable numerical technique.

4. Physical Description of Results

4.1. *Flow and temperature graphs*

Figures 2–6 are prepared to examine the behavior of velocity and temperature fields against various factors namely variable viscosity (Vogel's viscosity) parameter (A),

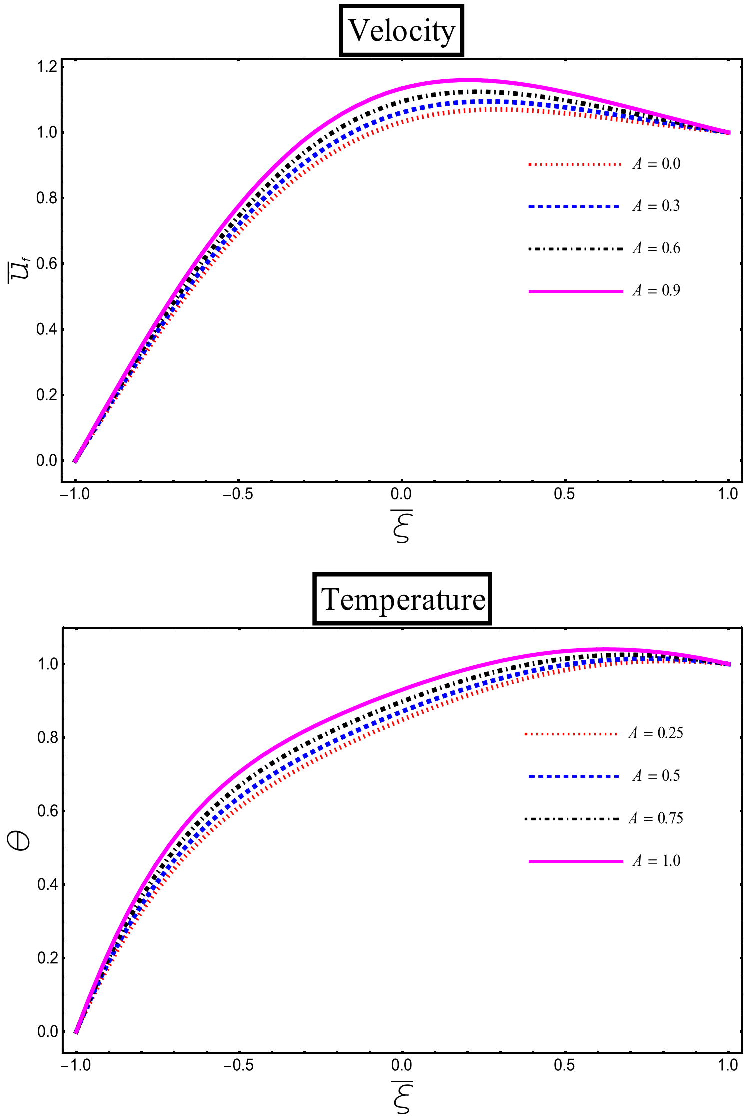

Fig. 2. (Color online) Variations in flow and temperature profiles via Vogel's viscosity parameter.

wall temperature parameter (θ_w), parameters (β_2) and (β_3) which defined variable magnetic field and thermal conductivity, respectively, and a dimensionless thermal radiation parameter (q). Figure 2 depicts that the increasing values of Vogel's viscosity parameter speed up the flow of fluid. This velocity increment is because of the radioactive heat flux effect, which decreases the viscosity and hence the fluid becomes thinner in this case. Similar effects of the Viscosity parameter on the temperature field are observed. The maximum height of the profile is noted near the moving wall. Figure 3 portrays the change in flow and temperature of fluid versus

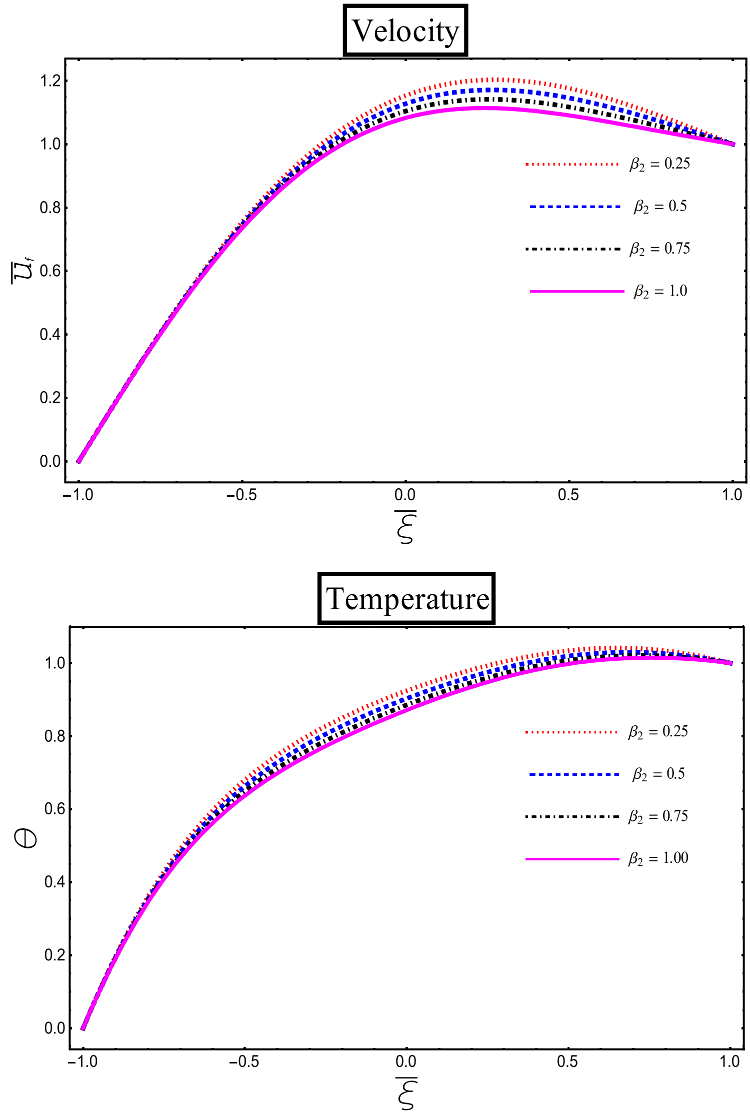

Fig. 3. (Color online) Variations in flow and temperature profiles via variable magnetic field parameter.

(β_2). When we enhance the variable magnetic field intensity, it causes a decrement in both velocity and temperature profiles. This is due to the fact that by increasing the magnetic field, the motion of fluid particles disturb as particles show attraction towards the magnetized region. The random motion of particles slows down the flow rate of fluid and in this way, kinetic energy also decreases which causes deceleration in temperature. These effects are more vivid near the right boundary which is the moving plate. The effects of wall temperature parameter (θ_w), on flow and

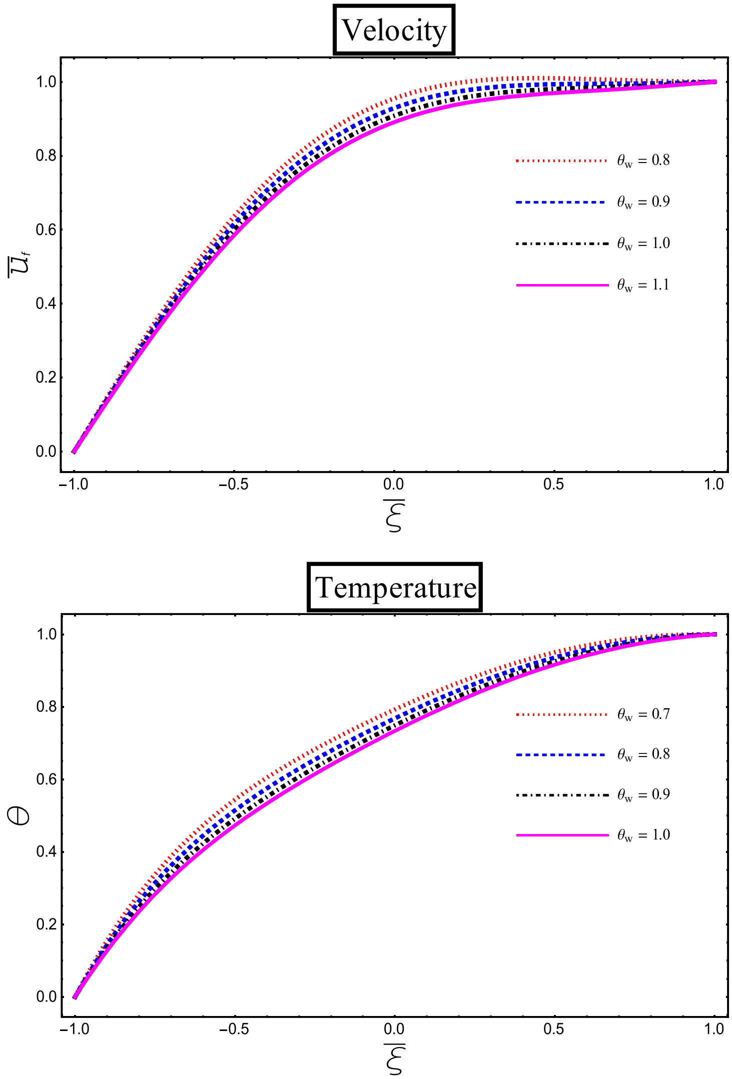

Fig. 4. (Color online) Variations in flow and temperature profiles via wall temperature parameter.

temperature are delineated in Fig. 4. These figures evaluated that altering values of (θ_w) slow down the fluid rate and also decelerated the temperature profile. This is obvious, as the wall temperature parameter creates accretion in the thermal slip parameter, which causes a decrement in mass and heat transmission. Even, when a small extent of heat is provided from the moving plate, it increases the thermal slip parameter which yields thickness in boundary slip. Figure 5 portrays that the increase in the magnitude of radiation parameter (q) speeds up the flow of fluid and also enlarges the temperature field. This is physically held as by increasing values of radiation parameter, the heat flux also increases which elevated the temperature

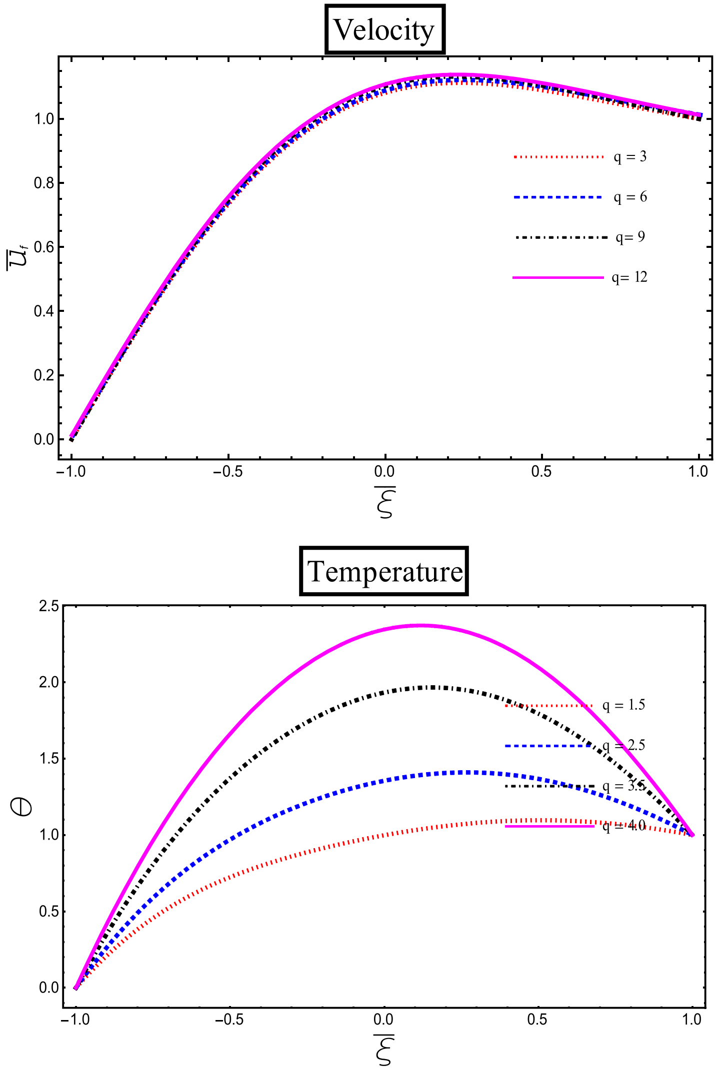

Fig. 5. (Color online) Variations in flow and temperature profiles via thermal radiation parameter.

field. Figure 6 exhibits that fluid velocity and temperature show reducing behavior versus variable thermal conductivity parameters. This is true, as higher thermal conductivity values create a better cooling solution by adjusting appropriate heat transfer and anticipated heat dissipation.

4.2. *Evaluation and verification of results*

In this section, we present a comparison between Newtonian and non-Newtonian fluids by sketching graphs (Fig. 7). Here, the length of the channel is an independent

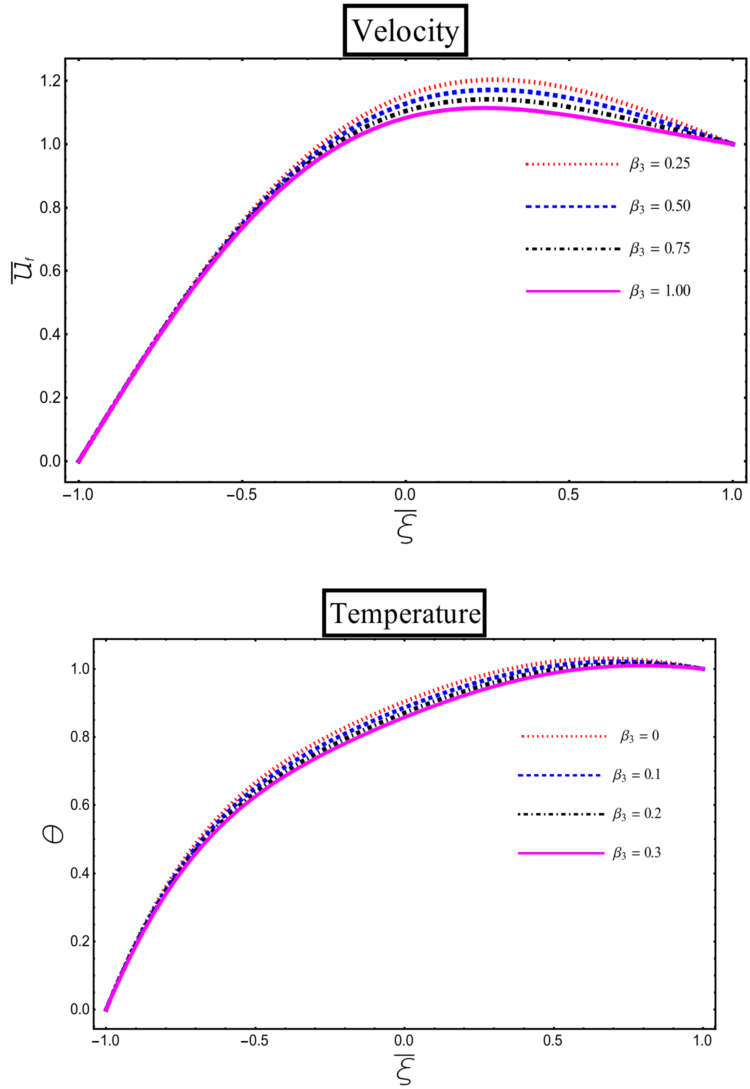

Fig. 6. (Color online) Variations in flow and temperature profiles via thermal conductivity parameter.

variable while velocity and temperature are dependent variables. From these figures, it is perceived that non-Newtonian fluid, which is couple stress fluid, shows elevation in height of velocity and temperature fields as compared to Newtonian fluid.

To verify our results with existing literature, we make a comparison of our results and Ellahi *et al.*[47] results in tabular form (Table 1 is organized for this purpose). Reynold's viscosity model is considered for this comparison. The results revealed that both results are well matched.

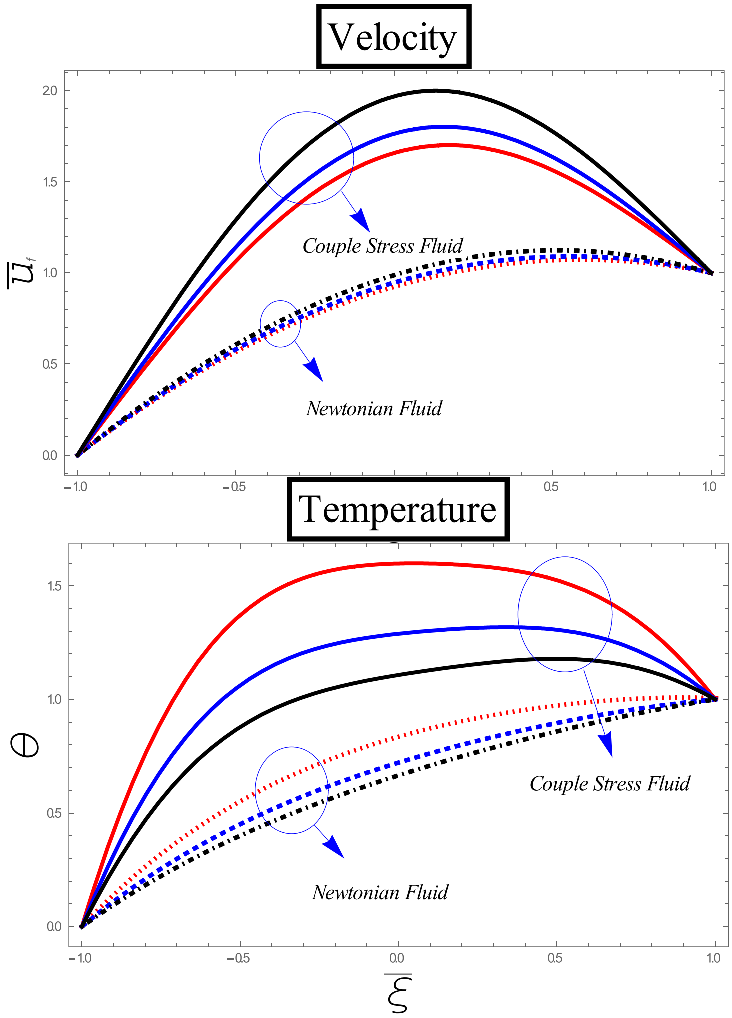

Fig. 7. (Color online) Evaluation between Newtonian and non-Newtonian fluids.

Table 1. Evaluation with the previous investigation for $\mu = e^{-\beta_1\theta}$ and $\beta_2 = \beta_3 = R_d = q = 0$.

	Ellahi *et al.*[47]		Our solution	
$\bar{\xi}$	u_p	u_f	$\bar{u}_p$	$\bar{u}_f$
−1	1.0	0.0	1.0	0.0
−0.6	1.3321	0.3221	1.3321	0.3221
−0.2	1.5826	0.5826	1.5826	0.5826
0.2	1.7698	0.7698	1.7698	0.7698
0.6	1.8998	0.8998	1.8998	0.8998
1	2.0	1.0	2.0	1.0

Table 2. Velocity of single and two-phase flows.

$\bar{\xi}$	$\bar{u}_f$ Single-phase ($\bar{C} = 0$)	$\bar{u}_p$ Solid–liquid phase ($\bar{C} = 0.4$)	$\bar{u}_f$ Solid–liquid phase ($\bar{C} = 0.4$)
−1	0.0	1.0	0.0
−0.6	0.59909	1.61393	0.61393
−0.2	0.99970	1.99616	0.99616
0.2	1.14738	2.11310	1.11310
0.6	1.11093	2.07374	1.07374
1.0	1.0	2.0	1.0

Table 3. Numerical data for temperature of fluid by taking different parameters.

$\bar{\xi}$	θ ($C = 0.4$)	θ ($M = 2$)	θ ($\beta_3 = 0.5$)	θ ($q = 0.5$)	θ ($R_d = 5$)
−1	0.0	0.0	0.0	0.0	0.0
−0.6	0.56189	0.31815	0.30391	0.41522	0.26050
−0.2	0.79441	0.60803	0.58175	0.76786	0.50620
0.2	0.93467	0.85779	0.82426	1.02351	0.72798
0.6	1.00860	1.060937	1.02706	1.16401	0.91883
1.0	1.0	1.0	1.0	1.0	1.0

The variations in single and two-phase flows at different grids of the domain by considering various parameters are presented in Table 2, and numerical data for temperature field versus several involved parameters is constructed in Table 3. It is found that the numerical results agree and satisfy all the corresponding conditions.

5. Conclusions

In this analysis, the Couette flow of non-Newtonian (couple stress) fluid with variable magnetic field and thermal conductivity effects is considered between walls of the channel. The upper wall of the channel is in constant motion while the lower wall is in a fixed position. The variable viscosity effects are also discussed by taking Vogel's viscosity case. A comparison between Newtonian and non-Newtonian fluids is presented by sketching graphs. This attempt is not just useful to investigate the mechanical and industrial multiphase flows but also delivers important results to fill the gap in the existing literature. The main outcomes of this investigation are as follows:

- The variable viscosity parameter elevated both velocity and temperature profiles.
- The wall temperature parameter slows down the flow of fluid and also declines the temperature.
- The variable thermal conductivity and variable magnetic field impede the velocity of the fluid and also retarded the temperature field.

- The thermal radiation parameter exhibits similar effects on velocity and temperature. It accelerated the velocity and temperature of the fluid.
- The maximum height of profiles is observed near the right boundary which is the moving wall of the channel.

This work will be supportive in the future to investigate bi-phase flows. We can extend this analysis by considering different geometries of multiphase Newtonian or non-Newtonian fluid flows with metallic particle suspensions.

Acknowledgment

The authors extended their appreciation to the Deanship of Scientific Research at King Khalid University, Abha 61413, Saudi Arabia for funding this work through research groups program under grant No. R. G. P-1/75/42.

References

1. Y. Chu *et al.*, *Int. Commun. Heat Mass Transfer* **120**, 105011 (2021).
2. Y. Chu *et al.*, *Int. Commun. Heat Mass Transfer* **119**, 104980 (2020).
3. I. H. Qureshi *et al.*, *Case Stud. Thermal Eng.* **26**, 101019 (2021).
4. M. M. Bhatti and A. Zeeshan, *Biomed. Eng. Lett.* **6**, 242 (2016).
5. M. Hatami, M. Khazayinejad and D. Jing, *Int. J. Heat Mass Transfer* **102**, 622 (2016).
6. T. Hayat *et al.*, *Results Phys.* **10**, 69 (2018).
7. K. Ramesh *et al.*, *Phys. Scr.* **96**, 025225 (2021).
8. M. Nazeer *et al.*, *Numer. Methods Partial Differ. Equ.* 1 (2021).
9. M. Nazeer *et al.*, *Int. Commun. Heat Mass Transfer* **124**, 105274 (2021).
10. N. Ali *et al.*, *Eur. Phys. J. Plus* **2**, 134 (2019).
11. H. Herwing and K. Gersten, *Warme Stoffubertrag* **20**, 7 (1986).
12. F. C. Lai and F. A. Kulacki, *Int. J. Heat Mass Transfer* **33**, 1028 (1990).
13. I. Pop, R. S. R. Gorla and M. Rashidi, *Int. J. Eng. Sci.* **30**, 1 (1992).
14. S. Manjunatha and B. J. Gireesha, *Ain Shams Eng. J.* **7**, 505 (2016).
15. S. L. Castañoa, B. J. Geurts and V. Armenio, *Int. J. Heat Fluid Flow* **81**, 108519 (2020).
16. H. A. Attia, *Mech. Res. Commun.* **26**, 115 (1999).
17. S. Ayub *et al.*, *Results Phys.* **7**, 3687 (2017).
18. M. Farooq *et al.*, *J. Assoc. Arab Univ. Basic Appl. Sci.* **14**, 9 (2013).
19. T. Hayat *et al.*, *Results Phys.* **7**, 518 (2017).
20. A. Khalid *et al.*, *Results Phys.* **9**, 1172 (2018).
21. M. Gholinia *et al.*, *Case Stud. Therm. Eng.* **13**, 100356 (2019).
22. S. O. Adesanya *et al.*, *J. Taiwan Inst. Chem. Eng.* **101**, 251 (2019).
23. B. Patel and V. Sardana, *Indian J. Tuberculosis* **67**, 277 (2020).
24. L. M. Srivastava, *Rheol. Acta* **25**, 638 (1986).
25. E. F. E. I. Shehawey and K. H. S. Mekheimer, *J. Phys. D, Appl. Phys.* **27**, 1163 (1994).
26. E. Walicki and A. Walicka, *Int. J. Appl. Mech. Eng.* **4**, 363 (1999).
27. R. Zahoor *et al.*, *Int. J. Multiph. Flow* **135**, 103530 (2021).
28. Y. J. Youn *et al.*, *Int. J. Multiph. Flow* **134**, 103470 (2021).
29. J. Zhang *et al.*, *Int. J. Multiph. Flow* **133**, 103456 (2020).
30. Y. Liu *et al.*, *Int. J. Multiph. Flow* **134**, 103497 (2021).
31. M. Nazeer *et al.*, *Surf. Interfaces* **22**, 100803 (2021).

32. H. Firdous *et al.*, *Phys. Scr.* **96**, 025803 (2021).
33. M. Nazeer *et al.*, *Surf. Interfaces* **22**, 100846 (2021).
34. M. Nazeer *et al.*, *Phys. Scr.* **96**, 015201 (2021).
35. N. Ashrafi and R. E. Khayat, *Phys. Fluids* **12**, 345 (2000).
36. M. Nazeer *et al.*, *Appl. Math. Mech.* (*Engl. Ed.*) **42**(1), 127 (2021).
37. M. Nazeer *et al.*, *J. Dispersion Sci. Technol.* (2021), doi:10.1080/01932691.2021.1877557.
38. H. Ge-JiLe *et al.*, *Adv. Mech. Eng.* **13**(1), 1 (2021).
39. C. K. W. Tam, *J. Fluid Mech.* **38**, 537 (1969).
40. F. Ahmad *et al.*, *Z. Naturforsch.* **75**, 225 (2020).
41. M. Nazeer *et al.*, *Int. Commun. Heat Mass Transfer* **117**, 104744 (2020).
42. M. Nazeer *et al.*, *J. Braz. Soc. Mech. Sci. Eng.* **41**, 518 (2019).
43. M. Nazeer *et al.*, *Z. Naturforsch.* **74**, 961 (2019).
44. M. I. Khan *et al.*, *Adv. Mech. Eng.* **12**(12), 1 (2020).
45. M. Nazeer *et al.*, *Numer. Methods Partial Differ. Equ.* 1 (2021).
46. M. Nazeer, *SN Appl. Sci.* **3**, 213 (2021).
47. R. Ellahi *et al.*, *Symmetry* **11**, 647 (2019).